Information-theoretic method for wavelength selection in bioluminescence tomography

Basevi, H.R.A.; Guggenheim, J.A.; Dehghani, H.; Styles, I.B.

DOI:
10.1117/12.2033320

Document Version
Peer reviewed version

Citation for published version (Harvard):
Basevi, HRA, Guggenheim, JA, Dehghani, H & Styles, IB 2013, Information-theoretic method for wavelength selection in bioluminescence tomography. in *Progress in Biomedical Optics and Imaging - Proceedings of SPIE.* vol. 8799. https://doi.org/10.1117/12.2033320

Information-theoretic method for wavelength selection in Bioluminescence Tomography

Hector R.A. Basevi,[1,2], James A. Guggenheim,[1,2] Hamid Dehghani,[1,2] and Iain B. Styles[2]

[1]PSIBS, University of Birmingham, Edgbaston, Birmingham, B15 2TT, United Kingdom;
[2]School of Computer Science, University of Birmingham, Edgbaston, Birmingham, B15 2TT, United Kingdom

ABSTRACT

Practical imaging constraints restrict the number of wavelengths that can be measured in a single Bioluminescence Tomography imaging session, but it is unclear which set of measurement wavelengths is optimal, in the sense of providing the most information about the bioluminescent source. Mutual Information was used to integrate knowledge of the type of bioluminescent source likely to be present, the optical properties of tissue and physics of light propagation, and the noise characteristics of the imaging system, in order to quantify the information contained in measurements at different sets of wavelengths. The approach was applied to a two dimensional simulation of Bioluminescence Tomography imaging of a mouse, and the results indicate that different wavelengths and sets of wavelengths contain different amounts of information. When imaging at a single wavelength, 580nm was found to be optimal, and when imaging at two wavelengths, 570nm and 580nm were found to be optimal. Examination of the dispersion of the posterior distributions for single wavelengths suggests that information regarding the centre of the bioluminescence distribution is relatively independent of wavelength, whilst information regarding the width of the bioluminescence distribution is relatively wavelength specific.

Keywords: Bioluminescence Tomography, Spectral Imaging, Optical Tomography, Wavelength Optimization, Information Theory, Mutual Information

1. INTRODUCTION

Bioluminescence Tomography (BLT)[1] is a pre-clinical medical imaging technique that quantifies the three-dimensional distribution of a bioluminescent molecule within tissue, via measurement of the light that reaches the surface of the subject. Bioluminescent molecules typically have a finite spectral range within which they emit,[2] and tissues have spectrally dependent scattering and absorption properties,[3] which suggests that measurements acquired at different wavelengths may provide different information about the bioluminescent sources. However, the strong attenuation of tissue, coupled with the relatively weak emission of bioluminescent molecules and limited imaging time (due to the length of time for which a subject can be safely kept sedated, and the consumption of the substrate of the bioluminescence process and subsequent reduction in bioluminescence), mean that it is typically not practical to image at all wavelengths that might be of interest. It is then necessary to choose a set of wavelengths at which to image such that a maximum amount of information about the bioluminescent sources is preserved.

Information Theory analyses the information content of signals.[4] Mutual Information (MI) is an information theoretic measure of the mutual dependence of two random variables which quantifies to what extent knowledge of the value of one random variable reduces our uncertainty of the value of the other random variable. It has been used for system optimisation in other contexts, such as detector placement[5] and laser modulation frequency[6] in Fluorescence Tomography. If the bioluminescence problem is viewed in this context, the distribution of all possible bioluminescence images forms one random variable, and the distribution of all possible measurements acquired at a particular wavelength set forms a second random variable. MI can quantify the degree to which

Further author information: (Send correspondence to Hector R.A. Basevi)
Hector R.A. Basevi: E-mail: hrb886@bham.ac.uk

measurements at a particular wavelength set reduces the uncertainty in the bioluminescence image, and vice versa. The expression for MI is:

$$I(X,Y) = \int_{y\in Y}\int_{x\in X} P(x,y)\log\left(\frac{P(x,y)}{P(x)P(y)}\right)\mathrm{d}x\,\mathrm{d}y \tag{1}$$

where x is a bioluminescence image drawn from the set of possible bioluminescence images X, y is a set of measurements drawn from the set of possible measurements Y, $P(x,y)$ is the joint probability of observing bioluminescence image x and measurements y together, and $P(x)$ and $P(y)$ are the probabilities of observing a bioluminescence image and measurement set respectively, independent of any observation of the other.

In this work Monte Carlo (MC) integration was used to estimate the value of $I(X,Y)$ in a two dimensional simulation for the set of bioluminescence images consisting of a spatially Gaussian bioluminescence source present somewhere in the tissue, and for measurement sets consisting of measurements taken at one or two wavelengths. The dispersion (in terms of standard deviation) of the posterior distribution (see eq. (6)) was also examined as a metric of the quality of the posterior distribution, to both provide more information about the distribution and act as a validation mechanism for MI. The results indicate that information content is wavelength-dependent, and that 580nm is the optimal measurement wavelength for a single wavelength set, while 570nm and 580nm are the optimal measurement wavelengths for two wavelength set. The dispersion of the posterior distribution agrees with the MI results for the single wavelength set, and indicates that the wavelength dependent information is predominantly related to the source width. However, the dispersion disagrees with the MI results in the two wavelength case.

2. METHODS

A finite element approach was used to model the bioluminescence problem. A two dimensional circular finite element mesh was generated with the Nirfast[7] software package, which was also used to model the physics of light propagation through tissue (see fig. 1). The optical properties of the circular mesh were assigned by overlaying the circular mesh onto a three dimensional mouse atlas containing labelled tissue types,[8] transferring the labels onto the circular mesh (see fig. 1a), and then using optical properties from literature[3] for each tissue type (see figs. 1c and 1d). Sixteen measurements locations (see fig. 1a) were placed on the edge of the mesh so as to emulate the surface coverage of an existing multi-modality imaging system including a camera and two mirrors.[9] The bioluminescence distribution within the mesh was chosen to be Gaussian (see fig. 1b). The bioluminescence source intensity and width were drawn from Normal distributions $\mathcal{N}(10, 2.8)$ and $\mathcal{N}(3\text{mm}, 0.25\text{mm}^2)$ respectively, and the source centre location was drawn from a Uniform distribution over the whole mesh.

The use of a camera constrains all measurements at a particular wavelength to share a common exposure time. For this study it was assumed to be possible to expose the camera until at least one measurement reached 90% of the capacity of the camera (which is 65535 counts) at any of the wavelengths examined. The measurement noise was modelled on the multi-modality imaging system, which has very low read noise on the order of 10 electrons, in addition to shot noise, which was approximated via a Normal distribution to reduce computational time.

MI was estimated through nested MC integration. The expression for MI (see eq. (1)) can be rewritten as:

$$I(X,Y) = \int_{y\in Y}\int_{x\in X} P(x,y)\log\left(\frac{P(y|x)}{P(y)}\right)\mathrm{d}x\,\mathrm{d}y \tag{2}$$

Equation (2) cannot be readily integrated analytically for the desired problem, and so its value was estimated using MC integration, which results in the following expression:

$$I(X,Y) \approx \frac{1}{N}\sum_{i=1}^{N}\log\left(\frac{P(y_i|x_i)}{P(y_i)}\right) \tag{3}$$

The variables x_i and y_i are samples drawn from the joint distribution $P(x,y)$. The probability distribution $P(y)$ is defined through $P(y|x)$ and $P(x)$:

$$P(y) = \int_{x\in X} P(y|x)P(x)dx \tag{4}$$

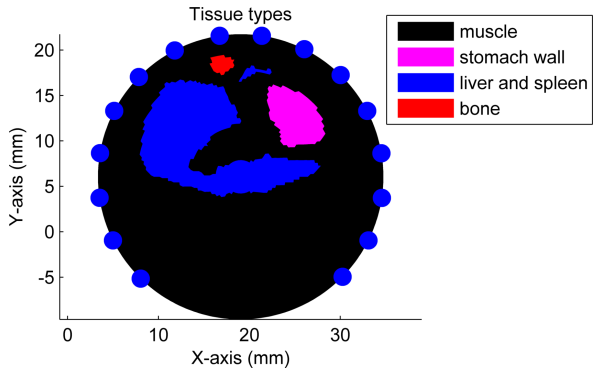

(a) Tissue types present within test mesh

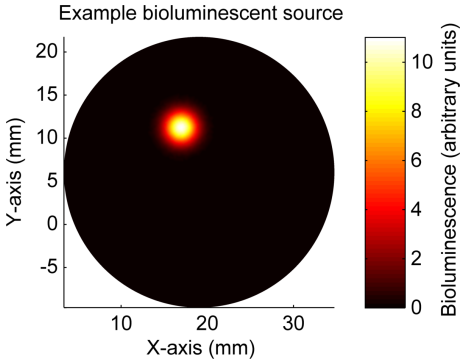

(b) Example bioluminescent source

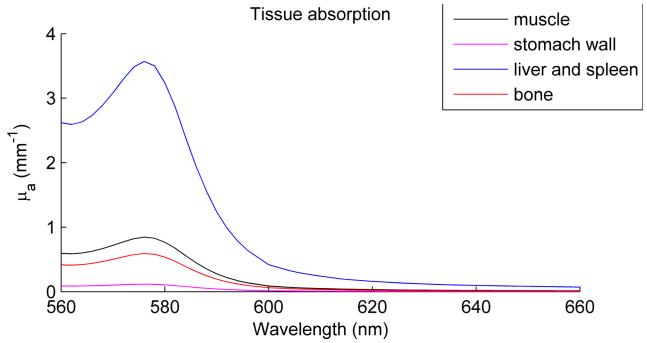

(c) Absorption spectrum of tissue types

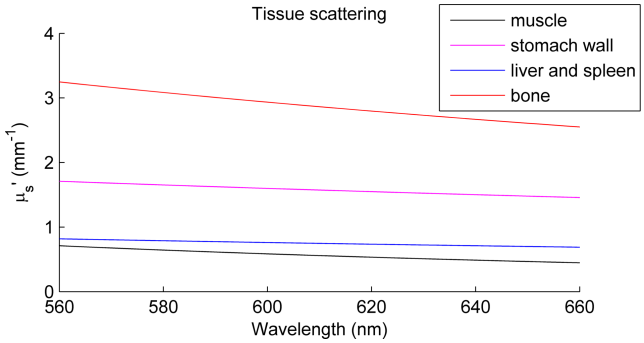

(d) Scattering spectrum of tissue types

Figure 1: Problem mesh and optical properties. Figure 1a shows the segmentation of the mesh into different tissue types. The blue circles on the edge of the mesh indicate detector locations. Figure 1b shows an example Gaussian bioluminescence distribution within the mesh. The graphs in figs. 1c and 1d show the spectral dependence of μ_a and $\mu_s\prime$, the absorption and reduced scattering coefficients respectively, for the different tissue types.

Unfortunately, eq. (4) is also not readily integrable, and so MC integration was also used to estimate the value of $P(y)$, resulting in the final expression:

$$I(X,Y) \approx \frac{1}{N}\sum_{i=1}^{N} \log\left(\frac{P(y_i|x_i)}{\frac{1}{M}\sum_{j=1}^{M} P(y_i|x_j)}\right) \tag{5}$$

The variable x_j is drawn from the distribution $P(x)$.

The computation of MI was implemented in Matlab and executed in a parallel manner on multiple computers. In single wavelength estimation, a total of 2.5×10^6 samples were used for each wavelength. In testing dual wavelength sets, a total of 7.5×10^6 samples were used for each wavelength set. It was assumed that surface signal at each wavelength is sufficient to allow the 16-bit camera to integrate until measurements fill 90% of its dynamic range.

The MI results were validated via an examination of the characteristics of the posterior distribution $P(x|y)$. Bayes' theorem states:

$$P(x|y) = \frac{P(y|x)P(x)}{P(y)} \tag{6}$$

It is impractical to evaluate the posterior in this case, so Markov Chain Monte Carlo (MCMC) sampling was used to draw samples from $P(x|y)$, which were then used to quantify posterior distribution properties such as the dispersion in terms of standard deviation of distribution centre, intensity and width for a number of

test problems. The dispersion gives an estimate of the width of $P(x|y)$ for the bioluminescence distribution parameters, as disperse distributions generally indicate a large degree of uncertainty.

3. RESULTS AND DISCUSSION

The results of MI estimation are presented in figs. 2 and 3. The single wavelength MI estimation in fig. 2 shows large differences in MI for different wavelengths, which indicates that measurement information content is wavelength-dependent. More information appears to be provided by lower wavelengths, despite the reduction in absorption and scattering at higher wavelengths (see figs. 1c and 1d). The wavelength with the strongest absorption, 580nm, appears to provide the greatest information (under the assumption that the camera is sufficiently sensitive that at least one measurement can reach 90% of the camera capacity). Indeed, the MI distribution appears to broadly follow the tissue absorption distribution (see fig. 1c). The dispersion of the posterior distributions in the form of the standard deviations produces mixed results here. The location standard deviation (see fig. 2b) does not strongly favour any wavelength, but if anything slightly favours high wavelengths in terms of the variation of standard deviation, and outliers. However, intensity standard deviations (see fig. 2c) favour 570nm and 580nm, and width standard deviations (see fig. 2d) strongly favour 580nm. This suggests that while 580nm may not necessarily provide the most information about bioluminescence distribution centre, it does provide the most information about distribution width and distribution intensity, such that it provides the most information overall.

The MI for sets of two wavelengths (see fig. 3a) indicate that a low wavelength is advantageous. However, MI changes little when changing a second higher wavelength, which indicates that the new information provided by measurements at a second wavelength is largely independent of the wavelength. The maximum MI here is associated with the wavelength set consisting of 570nm and 580nm. However, the validation via examination of posterior standard deviations is clearly in disagreement with MI here. For each of the variables (location, intensity, and width), the wavelength set consisting of 570nm and 580nm is not optimal. Wavelengths consisting of a wavelength below 590 and a wavelength above 600nm are superior in terms of standard deviation. It is not clear why this is the case, although it is possible that the posterior distribution for sets of two wavelengths is so complex that the distribution dispersion is not a good measure of the information content, or that the MCMC sampling method is not sampling from the full distribution.

4. CONCLUSIONS

MI was used as a criteria for wavelength selection in BLT, and validated by examination of the "width" of the posterior distribution. For single wavelengths, MI suggests that 580nm is optimal and that there is a significant difference in information content between wavelengths. Analysis of posterior distribution standard deviations suggests that this difference in information content is predominantly associated with bioluminescence distribution width, followed by intensity.

For sets of two wavelengths, MI suggests that the set consisting of 570nm and 580nm is optimal, although the MI distribution indicates that the lowest wavelength of the set provides the majority of the information and the choice of second wavelength is of much less importance. However, in this case the posterior distribution standard deviations disagree with MI, and suggest that the best wavelength sets consist of a wavelength below 590nm and a wavelength above 600nm. The reason for this discrepancy is unknown, although it is possible that the posterior distribution for sets of two wavelengths is sufficiently complex that either the distribution standard deviations are not a good measure of information content or the MCMC algorithm is not sampling from the full distribution. Future work should re-examine this issue to determine its source.

The presented results suggest that wavelength selection in BLT significantly affect the quality of the information obtained through imaging, and Mutual Information shows promise as a metric for optimal wavelength selection. In addition, MI can in principle be used to examine the effects of other imaging factors, such as detector location placement, optical property variation, and bioluminescent source location. Future work will examine these, with the goal of performing subject specific imaging optimisation.

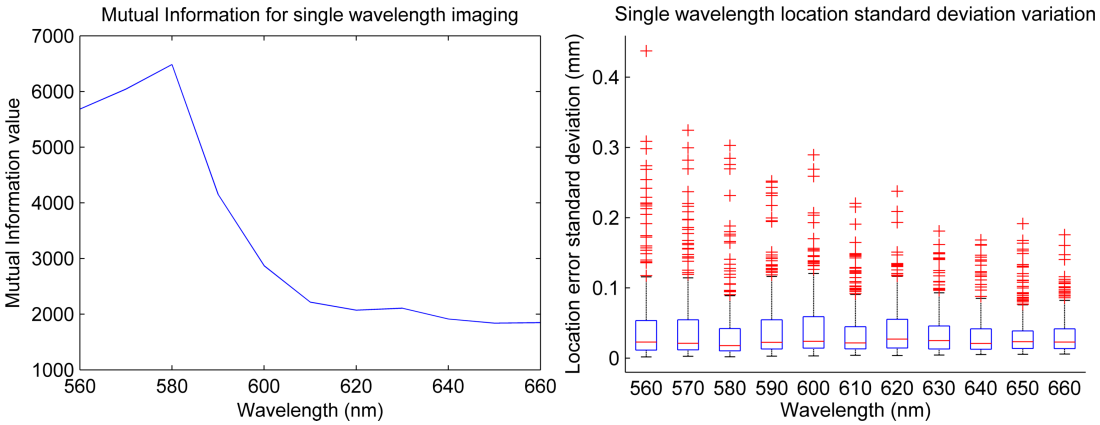

(a) MI for single wavelengths

(b) Source location error

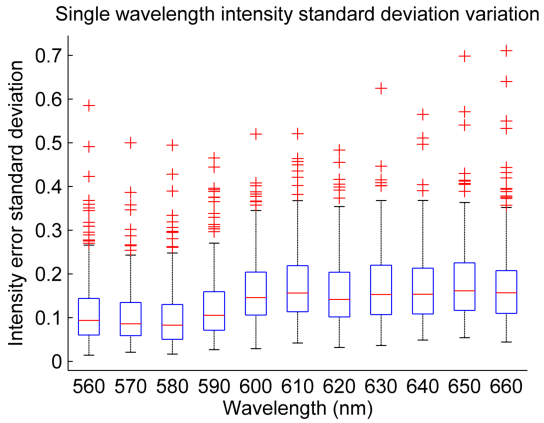

(c) Source intensity error

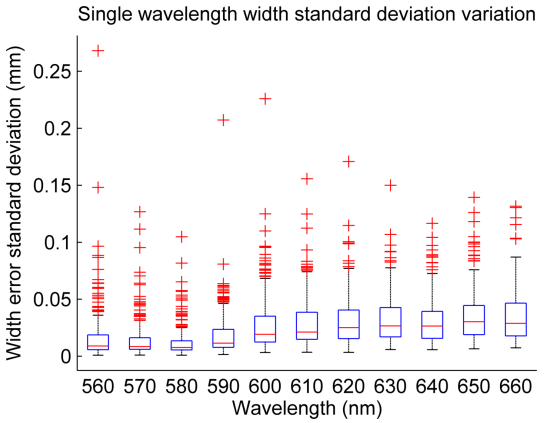

(d) Source width error

Figure 2: MI for single wavelengths. Figure 2a shows the MI for single wavelengths, estimated using a total of 2.5×10^6 samples, which indicate that 580nm is optimal. Figures 2b to 2d show the dispersion in terms of the standard deviations of the location, intensity and width samples from the posterior distribution respectively, in the form of box plots. The red line is the median of the distribution; the blue box shows the first and third quartile; the black lines show the limits of the data; the red crosses show outliers of the distribution. The location standard deviations do not display an obvious pattern (and if anything high wavelengths appear slightly better), but the intensity and especially the width standard deviations agree with the mutual information result, as the standard deviations are on average smaller, and in the case of width are more consistently smaller.

5. ACKNOWLEDGMENTS

Funding for this work was provided by EPSRC grant EP/F50053X/1 through studentships to Hector Basevi and James Guggenheim at the PSIBS Doctoral Training Centre at the University of Birmingham.

REFERENCES

[1] Kuo, C., Coquoz, O., Troy, T., Xu, H., and Rice, B., "Three-dimensional reconstruction of in vivo bioluminescent sources based on multispectral imaging," *J. Biomed. Opt.* **12**(2), 024007 (2007).

[2] Seliger, H. and McElroy, W., "Spectral emission and quantum yield of firefly bioluminescence," *Arch. Biochem. Biophys.* **88**(1), 136–141 (1960).

[3] Alexandrakis, G., Rannou, F., and Chatziioannou, A., "Tomographic bioluminescence imaging by use of a combined optical-pet (opet) system: a computer simulation feasibility study," *Phys. Med. Biol.* **50**(17), 4225 (2005).

[4] MacKay, D. J., [*Information theory, inference and learning algorithms*], Cambridge university press (2003).

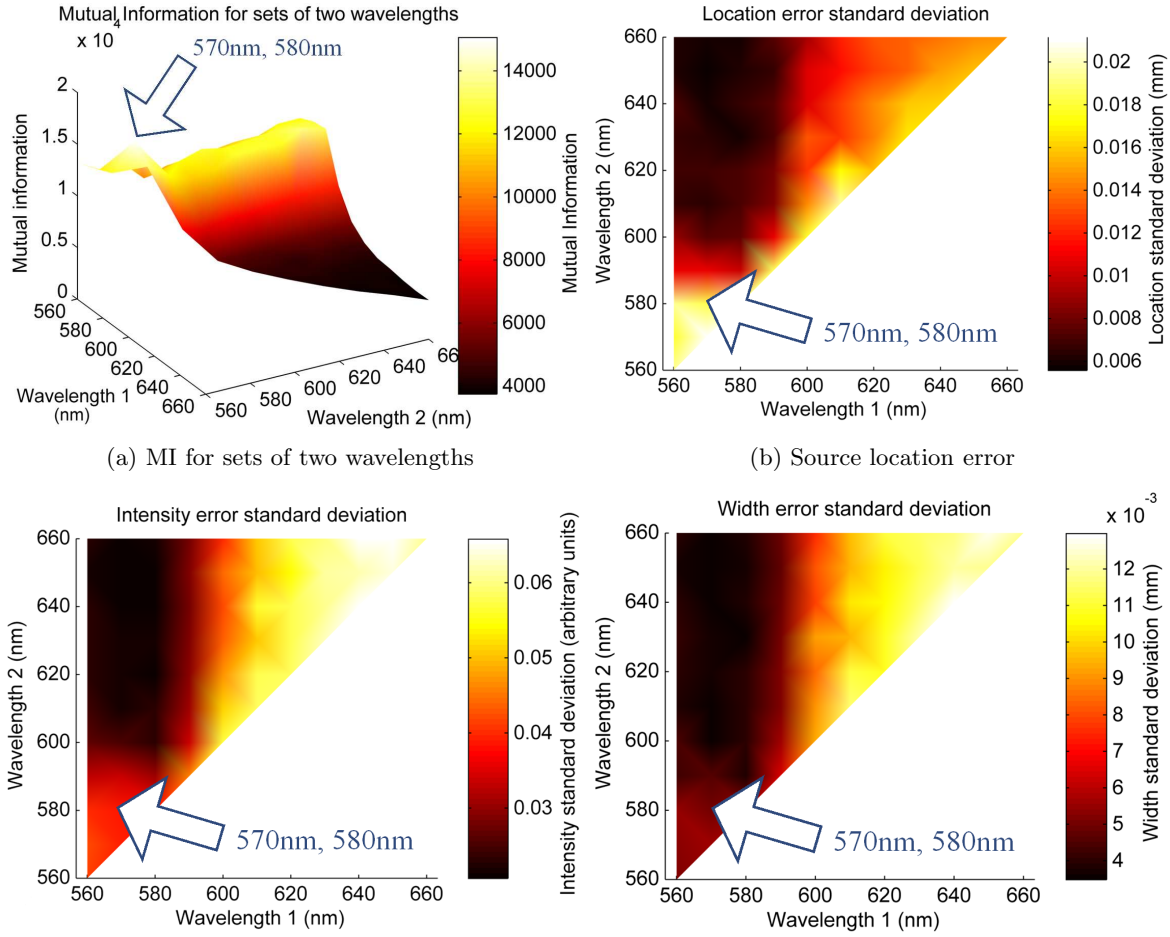

(a) MI for sets of two wavelengths

(b) Source location error

(c) Source intensity error

(d) Source width error

Figure 3: Figure 3a shows the MI for sets of two wavelengths, estimated using 7.5×10^6 samples. The primary pattern visible here is that wavelength sets with at least one low wavelength possess the highest MI. The second (higher) wavelength does not in general greatly alter the MI. The best wavelength set is that consisting of 570nm and 580nm. However, the posterior standard deviations do not agree with MI in this case. Figures 3b to 3d show the mean standard deviation for each of the wavelength sets, and indicate that the wavelength sets with lowest posterior standard deviations contain a wavelength below 580nm and a wavelength above 600nm.

[5] Freiberger, M. and Scharfetter, H., "Sensor optimization for fluorescence optical tomography by experimental design methods," in *Proc. SPIE*, **7174**, 717419 (2009).

[6] Milstein, A. B., Stott, J. J., Oh, S., Boas, D. A., Millane, R., Bouman, C. A., and Webb, K. J., "Fluorescence optical diffusion tomography using multiple-frequency data," *J. Opt. Soc. Am. A* **21**(6), 1035–1049 (2004).

[7] Dehghani, H., Eames, M., Yalavarthy, P., Davis, S., Srinivasan, S., Carpenter, C., Pogue, B., and Paulsen, K., "Near infrared optical tomography using nirfast: Algorithm for numerical model and image reconstruction," *Commun. Numer. Meth. En.* **25**(6), 711–732 (2009).

[8] Dogdas, B., Stout, D., Chatziioannou, A., and Leahy, R., "Digimouse: a 3d whole body mouse atlas from ct and cryosection data," *Phys. Med. Biol.* **52**(3), 577 (2007).

[9] Guggenheim, J., Basevi, H., Styles, I., Frampton, J., and Dehghani, H., "Multi-view, multi-spectral bioluminescence tomography," in *Biomedical Optics*, Optical Society of America (2012).